Enhancing the photon detection efficiency of Silicon Photomultipliers for RICH at ALICE 3

Katharina Metzger

supervised by Nicola Nicassio and Antonio Di Mauro

June 2nd to August 29th, 2025

1 RICH at ALICE 3

The ALICE Collaboration is proposing a new apparatus, ALICE 3, planned to be installed for LHC Run 5, to investigate the Quark Gluon Plasma properties beyond current limits. Studies for the development of a Ring-Imaging Cherenkov detector for charged particle identification in the barrel region with ALICE 3 are ongoing. The proposed layout is a proximity-focusing RICH, using aerogel as Cherenkov radiator and a layer of Silicon Photomultipliers (SiPMs) for the photon detection. The coupling of a thin fused silica window with refractive index of approximately 1.47 at 400 nm to the SiPM for precise charged particle timing is also under study.

The accompanying figure 1 shows the different components of RICH: the aerogel in blue, the gas in grey and the photodetector modules in orange. A limitation in the use of SiPMs comes from their limited radiation tolerance, leading to a dark count rate (DCR) increasing above the MHz/mm2 level during operation at the expected operation temperature and recommended overvoltage with the expected fluence levels. A study on the possibility of using smaller SiPMs coupled with respect to the $2{\times}2$ mm^2 baseline was done in order to reduce the dark count rate while retaining the same or even higher photon detection yield. A significant limitation to the SiPM photon detection efficiency (PDE) comes from reflections occurring at all SiPM interfaces among window, resin, passivation layer and silicon and leading to both photon losses and multiple-reflection background. Here, a study using a rough interface between the silicon window and the gas was conducted to reduce reflections.

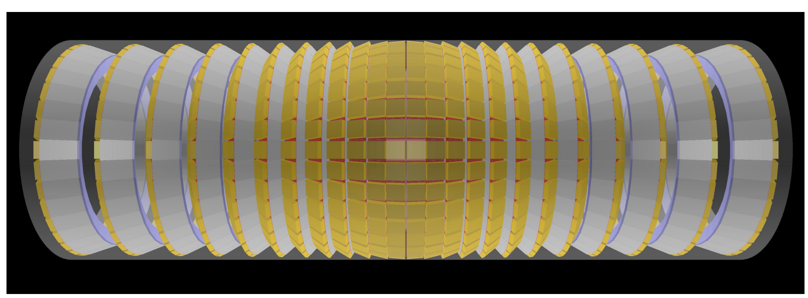

Figure 1: Schematic view of the barrel RICH (bRICH) detector.

2 Track and photon angular distributions at the bRICH SiPMs

Studies on the track and photon angular distributions were conducted to determine the most relevant angle ranges for optimization purposes. Using Pb-Pb collisions at 5.52 TeV, the ost populated angular regions can be obtained from figure 2 and 3. Especially relevant for the rest of this report is figure 3 which shows that the most relevant incidence angle region lies below 34 degrees with a peak around 16 degrees.

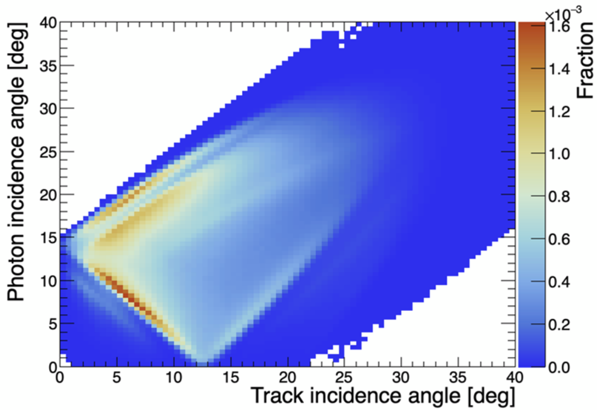

Figure 2: 2D-histogram of the track and incidence angles for photons produced in Pb-Pb collisions.

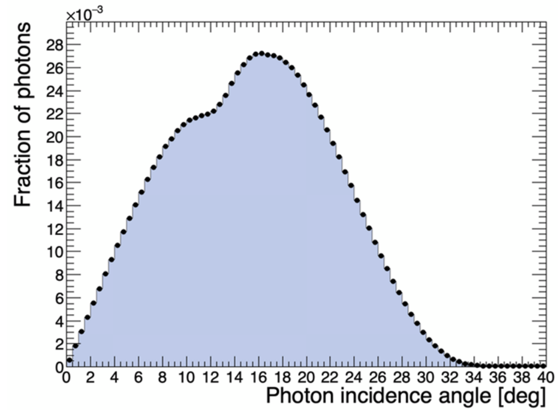

Figure 3: 1D-histogram of the incidence angle for photons produced in Pb-Pb collisions.

3 Light concentrators

The idea of light concentrators to mitigate radiation damage effects using smaller SiPMs was proposed. Since the dark count rate scales linearly with the surface area of the SiPMs, minimizing the size of the SiPMs directly improves the data. Truncated pyramids made of fused silica (n $\approx$ 1.47 at 400 nm) with a larger base of 2.2$\times$2.2 mm^2 and a smaller base of 1$\times$1 mm^2, as shown in figure 4, lead to a factor 4 reduction in radiation damage effects. At the same time, they increase the photon detection yield at small angles by 20% with respect to the baseline, assuming that the concentrators can be placed gaplessly. Originally, 2$\times$2 mm^2 SiPms with a 2.2$\times$2.2 mm^2 pitch were used, out of a need to consider the required interspace between contiguous SiPMs.

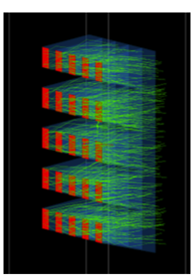

Figure 4: Light concentrators with SiPMs in red, concentrators in blue and photons tracks in green.

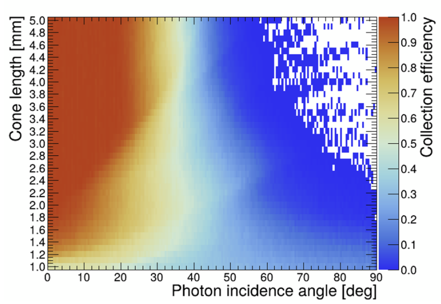

Figure 5: A scan over different concentrator length as shown on the left, showing the largest improvement for smaller angles at a length of 3.8 mm.

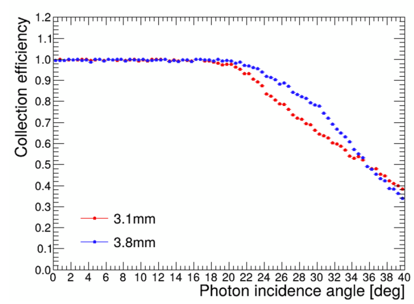

Figure 6: The collection efficiency versus the photon incidence angle for concentrators of length 3.8 mm and 3.1 mm

As a first part to this project, an optimization study of the length of the concentrator was conducted as shown in figure 5, yielding an improvement as shown in figure 6 for the optimum length of 3.8 mm in the angular region of interest.

A full simulation of RICH as shown in figure 7 using pions and electrons as primary particles was then performed to study the detection of photons depending on their origin: the aerogel, the gas, planned to be used to enhance electron identification, or the concentrators. Figure 7 shows an event display for an incident electron at 3 GeV/c. The larger Cherenkov cone is due to direct photons emitted created in the aerogel, on top of the background due to Rayleigh scattering, while the smaller cone is due to photons emitted in the gas. Further Cherenkov photons are produced inside the concentrators, representing a source of background to the gas-cluster based identification of electrons.

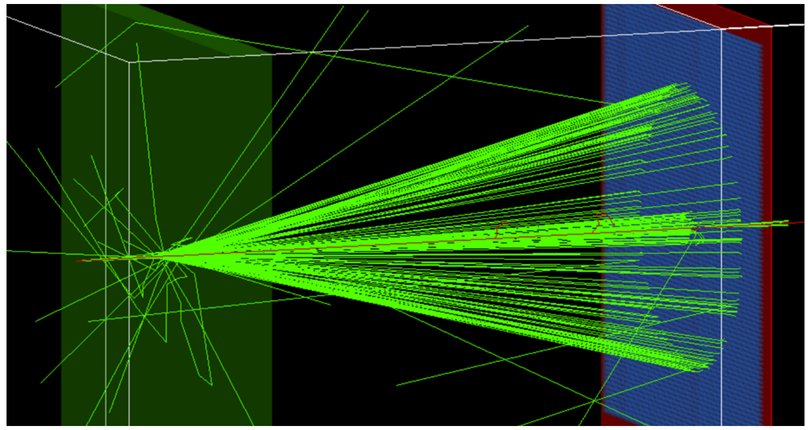

Figure 7: The full simulation showing the aerogel in dark green, the concentrators in blue, the SIPMs in red, the primary particle in dark red and the photons tracks in light green.

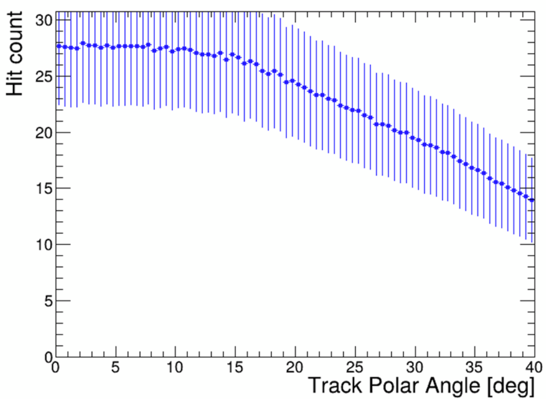

Figure 8: Mean number of SiPMs with a signal due to aerogel photons as a function of the track incidence angle in the configuration with concentrators. Poisson error bars are shown.

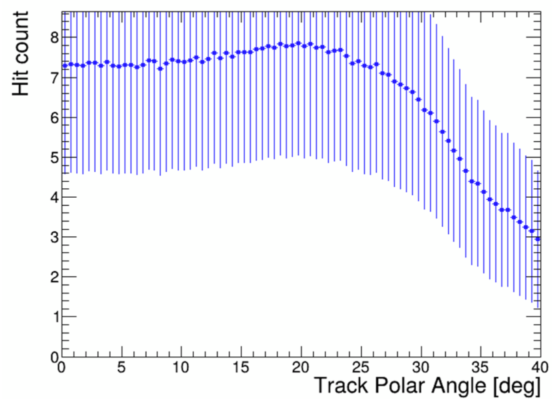

Figure 9: Mean number of SiPMs with a signal due to gas photons as a function of the track incidence angle in the configuration with concentrators. Poisson error bars are shown.

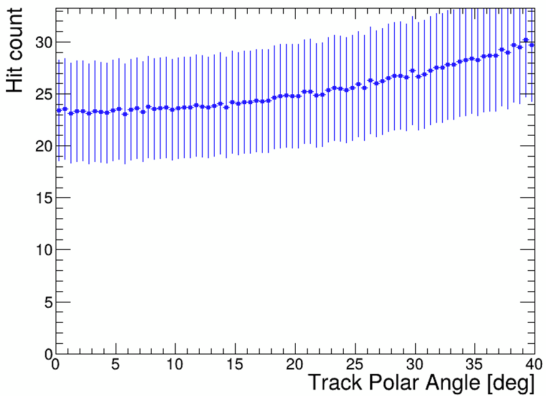

Figure 10: Mean number of SiPMs with a signal due to aerogel photons as a function of the track incidence angle in the configuration without concentrators. Poisson error bars are shown.

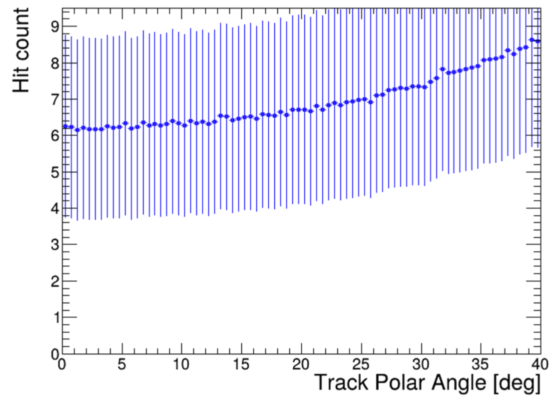

Figure 11: Mean number of SiPMs with a signal due to gas photons as a function of the track incidence angle in the configuration without concentrators. Poisson error bars are shown.

Figures 8-11 show the average number of SiPMs per event in which a signal is detected. Both the aerogel and the gas produce photons that are of interest, show higher values of hit count for lower angles. Aerogel photons of angles smaller than 20 degrees, show a better detection efficiency for a geometry with concentrators while for gas photons the concentrators are preferable up to about 25 degrees. The photons produced in the concentrators as shown in figure 13 represent a background to threshold-based electron ID using photon clusters from gas.

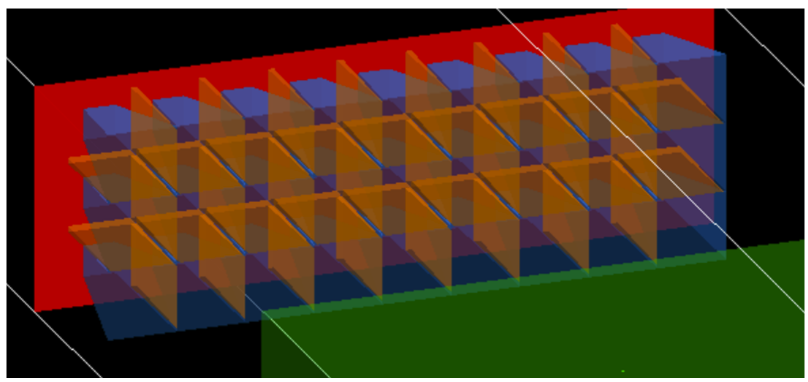

Figure 12: The concentrators with absorbers with the green concentrators in blue, the SiPMs in red, and absorbers in orange.

To further lower the concentrator photon detection, absorbers were introduced between the concentrators to stop photons that were produced in one concentrator from moving to another. The simulated geometry can be seen in figure 12. The simulation was run using optical photons around 400 nm at angles between 0 and 40 degrees. Figure 14 shows the resulting hit count per event, showing a reduction compared to the case of concentrators without absorbers in figure 13 of a factor up to 4 at low angles.

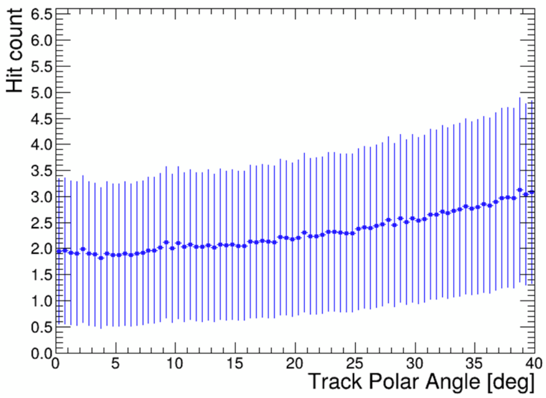

Figure 13: Concentrator photon hits versus the angle at the concentrator surface, without absorbers.

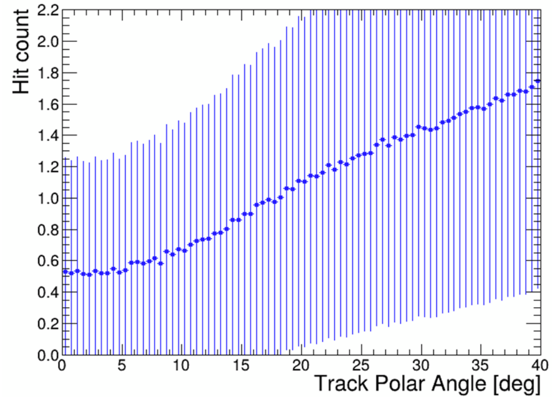

Figure 14: Concentrator photon hits versus the angle at the concentrator surface, with absorbers.

4 Rough silica window surface

In the hypothesis of integrating charged particle timing measurements in the bRICH, by coupling a thin fused silica window to the SiPMs, a limitation comes from photon reflections at the window surface. Reflection on the outer surface poses a problem to the detection of incoming photons. Equally, the reflective surface can trap both concentrator background photons and reflected data photons. The so introduced multiple reflections of aerogel or gas photons can result in hits in neighboring SiPMs representing a source of background. To counteract these reflections, a structured surface of the silicon window was investigated with optical photons. With the Glisur model in Geant4, a polished surface, a rough surface and an intermediate case were implemented. The results for these three scenarios both for entering and exiting photons are displayed in figures 15-20, with the first row showing the entering photons and the second row showing those that exit.

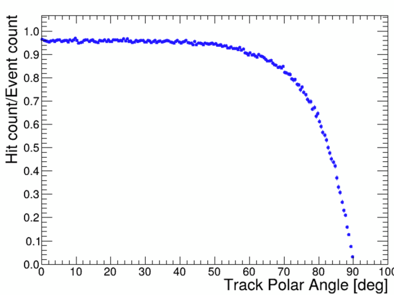

Figure 15: Fraction of impinging photons at the interface between gas and fused silica window that are transmitted assuming a polished surface.

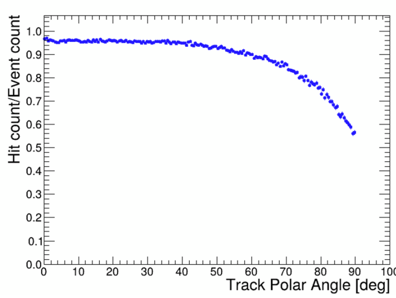

Figure 16: Fraction of impinging photons at the interface between gas and fused silica window that are transmitted assuming a surface with intermediate roughness.

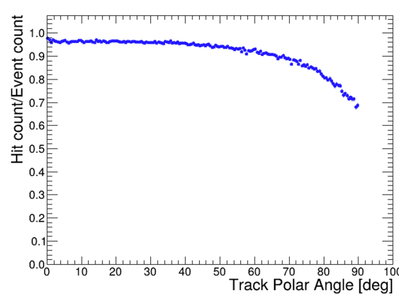

Figure 17: Fraction of impinging photons at the interface between gas and fused silica window that are transmitted assuming a surface with maximum roughness.

A higher collection efficiency for the entering photons means less reflection at the outer silicon surface, both of which are desirable for the experiment. Lower reflectance at the interface between gas and window results in a higher collection efficiency for the entering photons, as desirable for the experiment. Figures 15-17 show that for a higher roughness value the collection efficiency increases or stays approximately the same depending on the incidence angle at the surface.

For the exiting photons, a higher photon collection efficiency is undesirable as it leads to a larger background. Since most background photons in the silica window are created at an angle of 45 degrees, the collection efficiency for angles closer to 45 degrees is most important to be decreased. As shown by figures 18-20 this is the case for the roughest surface on the right. The downside to this is that the surface shows an increased reflectiveness for angles

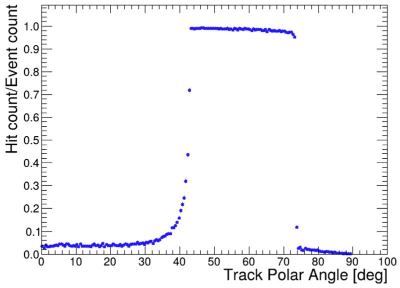

Figure 18: Fraction of photons reflected at the interface between the fused silica window and the SiPM that are reflected back at the interface between fused silica window and gas assuming a polished surface.

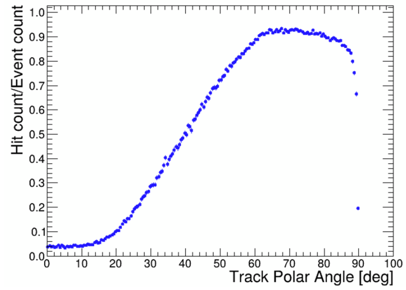

Figure 19: Fraction of photons reflected at the interface between the fused silica window and the SiPM that are reflected back at the interface between fused silica window and gas assuming a surface with intermediate roughness.

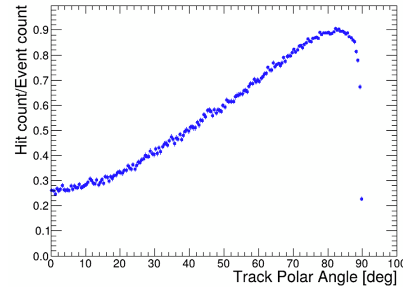

Figure 20: Fraction of photons reflected at the interface between the fused silica window and the SiPM that are reflected back at the interface between fused silica window and gas assuming a surface with maximum roughness.

up to 40 degrees, at which for example reflected aerogel photons are located.

5 Outlook

A different possible implementation of a rough silica window to gas interface could be achieved using anisotropic pyramids as shown in figure 21.

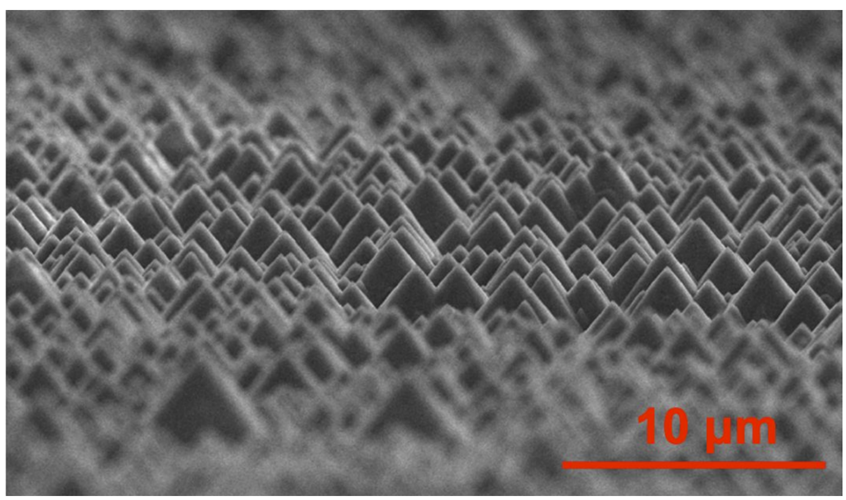

Figure 21: A different potential roughness implementation.